Deformation of the cell nucleus under indentation: Mechanics and mechanisms

A. Vaziri[a),b)]
Division of Engineering and Applied Sciences, Harvard University, Cambridge, Massachusetts 02138
H. Lee[b)]
Department of Mechanical Engineering and Biological Engineering Division, Massachusetts Institute of Technology, Cambridge, Massachusetts 02139
M.R. Kaazempur Mofrad
Department of Bioengineering, University of California, Berkeley, California 94720

(Received 21 December 2005; accepted 5 June 2006)

Computational models of the cell nucleus, along with experimental observations, can help in understanding the biomechanics of force-induced nuclear deformation and mechanisms of stress transition throughout the nucleus. Here, we develop a computational model for an isolated nucleus undergoing indentation, which includes separate components representing the nucleoplasm and the nuclear envelope. The nuclear envelope itself is composed of three separate layers: two thin elastic layers representing the inner and outer nuclear membranes and one thicker layer representing the nuclear lamina. The proposed model is capable of separating the structural role of major nuclear components in the force-induced biological response of the nucleus (and ultimately the cell). A systematic analysis is carried out to explore the role of major individual nuclear elements, namely inner and outer membranes, nuclear lamina, and nucleoplasm, as well as the loading and experimental factors such as indentation rate and probe angle, on the biomechanical response of an isolated nucleus in atomic force microscopy indentation experiment.

I. INTRODUCTION

The nucleus of eukaryotic cells is a site of major metabolic activities, such as DNA replication, gene transcription, RNA processing, and ribosome subunit maturation and assembly. It is separated from the cytoplasm by the nuclear envelope, which is composed of an outer nuclear membrane, inner nuclear membrane, nuclear pore complexes, and nuclear lamina. The inner and outer membranes are each a lipid bilayer separated by an electron-transparent region of approximately 10–40 nm. Nuclear lamina, which appears as a meshwork structure underneath the inner nuclear membrane, is thought to play a critical role in maintaining the structural integrity of the nucleus, and in organizing the nuclear envelope by recruiting proteins to the inner nuclear membrane and providing anchorage sites for chromatin.[1–3] Cytoskeleton-mediated deformation of the nucleus appears as a possible mechanotransduction pathway through which shear stress may be transduced to a gene-regulating signal.[4–7] In addition, nuclear envelope stiffness is proposed to be a regulator of force transduction on chromatin and genetic expression.[8,9] Recent observations by Deguchi et al. suggest the nucleus as a compression-bearing organelle,[10] emphasizing the importance of understanding the biomechanics of force-induced nuclear deformation.

Each of the above-mentioned nuclear elements has a distinct structure, which should be distinguished when studying the nucleus response to mechanical stimuli. Here, we develop a computational model based on finite element methods to simulate the response of an isolated nucleus to mechanical stimuli. In constructing this structural model for the nucleus, three distinct structural elements are considered: the double lipid bilayer, the cortical layer composed largely of lamin (nuclear lamina), and the nucleoplasm. The proposed finite element model is able to distinguish the structural role of individual nuclear elements, which is vital for understanding the nuclear mechanics and for functional insight. We have used this computational model to study the mechanics and mechanisms of deformation of an isolated nucleus

[a)]Address all correspondence to this author.
e-mail: avaziri@deas.harvard.edu
[b)]These authors contributed equally to this work.
DOI: 10.1557/JMR.2006.0262

under micropipette aspiration.[11] The model, validated using experimental observations of Guilak et al.,[14] was used to study nuclear mechanics in micropipette aspiration experiments. The results demonstrated that the overall response of an isolated nucleus in micropipette aspiration experiment is highly sensitive to the stiffness of the nuclear envelope, while the mechanical contribution of the nucleoplasm over the time course of these experiments is insignificant. Here, we used this computational model to examine the deformation of an isolated nucleus in indentation experiments using atomic force microscopy (AFM), which have been used extensively for imaging and studying the mechanical behavior and rheology of polymers,[13–16] thin films,[17–20] and biological materials.[21–24] It is noteworthy that the current data on the apparent stiffness of cell nuclei are rather divergent, with values ranging from 18 Pa to nearly 10 kPa[12,25–27] due to factors such as cell type, measurement techniques and conditions, length scale of interest, and also interpretation methods. The proposed computational model can help us to elucidate this apparent discrepancy.

Systematic analysis was carried out to understand the role of major individual nuclear elements, namely nuclear inner and outer membranes, nuclear lamina, and nucleoplasm, as well as the loading and experimental factors such as indentation rate and probe angle on the biomechanical response of an isolated nucleus in AFM indentation experiments. In addition, sharp probe AFM indentation experiments were conducted on isolated nuclei extracted from mouse embryo fibroblasts to establish the validity of the computational model.

II. COMPUTATIONAL MODEL FOR NUCLEUS MECHANICS IN ATOMIC FORCE MICROSCOPY INDENTATION

The nucleus can be efficiently modeled as a continuum media if the smallest length scale of interest is much larger than the distance over which nuclear structure or properties may vary. For example when the whole-nucleus deformations is considered, the length scale of interest is at least one order of magnitude larger than the space between the microstructural architecture involving packed chromatins, and therefore continuum description may be appropriate. In essence, the continuum mechanics is a coarse-graining approach that considers the local microscopic stress–strain relationship with averaged constitutive laws that apply at the macroscopic scale.

A. Details of the computational model

An axisymmetric model of the nucleus was developed, inspired by the actual geometry of a typical isolated nucleus of mouse embryo fibroblast plated on a slide glass substrate visualized using two-photon microscopy [Fig. 1(a)]. The nuclear membranes (inner and outer membranes) and the nuclear lamina had constant thickness of 7.5 and 25 nm,[28] respectively, i.e., the total thickness of the nuclear envelope is 40 nm [Fig. 1(b)]. The perinuclear space between the inner and outer nuclear membranes was not included due to its relatively structure-free composition,[29] speculating that the fluid-like content of this space freely escapes from the high-stress region at the early stage of indentation. No slippage was allowed at the interface between the nuclear lamina and the nucleoplasm, as well as the interface between the inner nuclear membrane and nuclear lamina, while the interface between the outer membrane and

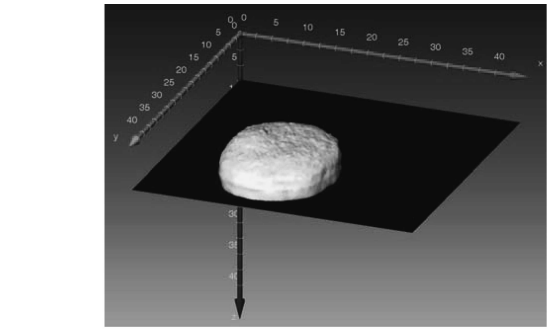

(a)

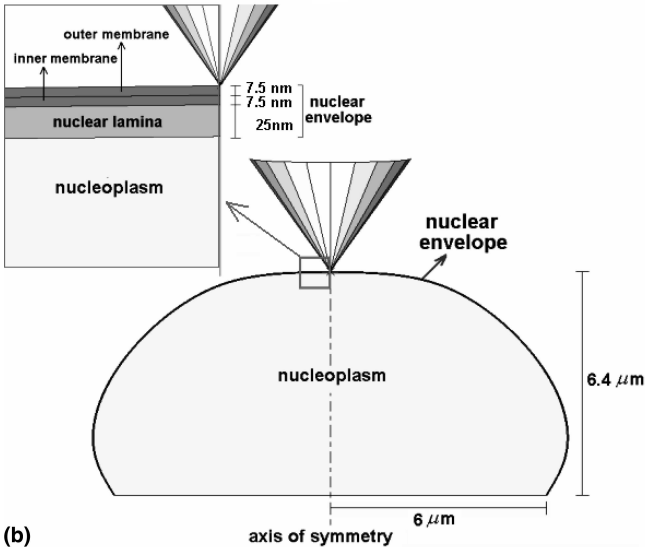

(b)

FIG. 1. (a) Two photon microscope image of an isolated nucleus extracted from mouse embryo fiberblast and plated on a glass substrate (black in the image) with the axes in micrometers. A 100× objective (numerical aperture 1.0, water) was used to acquire a 12.8 μm z-stack of eighty 16-bit 256 × 256 pixel images in the two-photon confocal microscope. Three-dimensional images of the isolated nucleus was reconstructed from the eighty z-stack image. (b) Computational model developed using the actual geometry of a typical isolated nucleus of mouse embryo fibroblast visualized using two-photon microscopy. (a) The tip of the AFM probe is modeled as a rigid sharp surface.

inner membrane is free to slide without friction. These contact conditions were adopted based on relatively well-known interactions of lamin-chromatin connections[30] and Emerin and Lamin B receptors (LBR) with Lamin A/C and Lamin B of the nuclear lamina.[31,32] The AFM tip was modeled as a rigid sharp surface with frictionless contact between the probe and the outer nuclear membrane. It is noteworthy that the AFM tip radius is not incorporated in the subsequent computations; however, we found that tip radius of 50 nm, which is considerably smaller than the indentation displacements of interest in this study, does not significantly alter the response of a cell nucleus and the associated stress distributions. Constant velocity of indentation was imposed to the probe as in the experiments (see Sec. III). Furthermore, a zero-displacement boundary condition was imposed at the bottom surface; i.e., the nucleus was attached to a rigid substrate.

The computations were performed using a commercially available finite element modeling software ABAQUS/Standard (Hibbit, Karlsson and Sorensen Inc., Providence, RI). Eight-node biquadratic axisymmetric finite elements were used in calculations for both nucleoplasm and nuclear envelope layers. A mesh sensitivity study was conducted to ensure the independence of the results from the computational mesh.

To examine the specific contribution of the nuclear envelope in the mechanics of nuclear deformation under AFM indentation, simulations were also performed using our computational model but excluding the nuclear envelope. The model without the membrane was an axisymmetric linear elastic model with the height and radius equal to 5 μm. A zero-displacement boundary condition was imposed at the bottom surface. The simulations are carried out using ABAQUS/Explicit (Hibbit, Karlsson and Sorensen Inc., Providence, RI) by employing an adaptive mesh generation scheme to prevent excessive deformation of the elements at large indentation.

B. Material specification

Elastic or viscoelastic descriptions of the nuclear elements, associated with its solid- and fluidlike dual characteristics, can be incorporated in the present computational model based on the dynamic time scale of interest. Here, the nucleoplasm is represented by viscoelastic Maxwell model with single characteristic time, analogous to a spring and a dashpot in series, which is consistent with our previous experimental observations.[33] The elastic modulus and characteristic time associated with the material model of the nucleoplasm are denoted by E and τ, respectively. Here, the baseline Maxwell model constants of the nucleoplasm were taken as $E = 25$ Pa and $\tau = 1$ s. The role of material constants associated with nucleoplasm material model on the overall response of the isolated nucleus under sharp probe indentation is discussed in Sec. IV. B.

Because AFM indentation experiments on nuclei are generally performed at time scales significantly lower than characteristic time associated with the viscoelastic nature of the nuclear envelope, different layers of nuclear envelope are modeled as linear elastic material, with K_b and K_{NL} denoting the bending stiffness of each lipid bilayer and nuclear lamina, respectively. Under this condition, the nuclear envelope exhibits an elastic response characterized by its apparent initial elastic modulus. Based on our own results and the results of others,[8,34] the baseline elastic properties of the lipid bilayers and nuclear lamina were taken as $K_b = 1.8 \times 10^{-19}$ N·m and $K_{NL} = 3.5 \times 10^{-19}$ N·m. Both nucleoplasm and nuclear envelope layers are assumed nearly incompressible. Here, we hypothesize that all the nuclear elements have equal value of Poisson's ratio denoted by ν. The effect of nuclear elements' Poisson's ratios on the overall response of an isolated nucleus in indentation experiment is discussed briefly in Sec. IV. B. It should be noted that in the present model, the effects of fluid expulsion from the nucleus are reflected by incorporating a Poisson's ratio that allow for some degree of compressibility. A realistic model of these effects would have to include fluid leakage through the pores that is both pressure- and time-dependent.

III. INDENTATION EXPERIMENT ON ISOLATED NUCLEI

Nuclei were extracted from mouse embryo fibroblasts cells by a nonionic detergent treatment as described previously[35] with the following modifications. Cells were washed with PBS and lysed in buffer A, which consisted of 0.1% Triton X-100, 10 mM ethylene diamine tetraaccetic acid (EDTA), 10 mM ethylene glycol tetraaccetic acid (EGTA), 10 mM KCl, and 10 mM 4-(2-hydroxyethyl)-1-piperazineethanesulfonic acid (HEPES) for 10 min in ice. Separation of nuclei from the cellular debris was attained by centrifugation at 1200 rpm for 10 min. Isolated nuclei were plated on the prepared glass, which was fit to the sample stage of the multimode scanning probe microscope (Veeco Instruments Inc., Woodbury, NY) and kept in PBS solution using a specialized probe holder. The probe was a silicon nitride cantilever (Veeco Instruments) with a pyramidal tip probe having a stiffness of 0.03 N/m. The AFM tip approaches the nucleus, as the stage is translated by piezoelectric material. The tip deflection is measured by calibrating the output voltage of the photodiode, which detected the laser spot reflected off the AFM probe and is converted to the force magnitude. For data acquisition, both the displacement of the stage and the deflection of the tip were recorded in every 8.8 nm translation of the piezoelectric

stage during indentation. Isolated nuclei sitting on the substrate, visualized using two-photon microscopy in three-dimensional (3D) coordinates [Fig. 1(a)], had approximately hemispherical shape in 3D coordinates. The AFM indentation was performed on the center region of nuclei plated on the prepared glass to minimize possible sliding during indentation. No difference was observed in force–indentation curves of repetitive indentations at the same position of the nucleus, which may imply that no sliding occurred during the course of the experiment. Dimensions of the AFM probe tip were obtained from images at 11,000× using a scanning electron microscope (SEM; JSM-5910, JEOL Inc., Peabody, MA). The probe tip utilized in all the experimental results presented here was approximately 3.5 μm tall with an end radius of ~50 nm and half angle of 35°. Total indentation depth was limited to 1.1 μm.

IV. RESULTS

The overall computational model of the isolated nucleus was used to study the mechanisms and mechanics of nuclear deformation under sharp probe indentation and to highlight the structural role of individual nuclear elements on the overall response in indentation experiment.

A. Importance of considering the membrane layer

To highlight the importance of considering the nuclear envelope when studying the overall deformation of an isolated nucleus under indentation, two sets of simulations were carried out using our computational models of an isolated nucleus, with and without the nuclear envelope. The details of the computational model are discussed in Sec. II. A. It is noteworthy that the model without the nuclear envelope effectively simulates the Hertz contact model[36,37] while incorporating the large-deformation effects. The displaced configuration of the nucleus model without membrane at the sharp probe displacement of 1 μm is depicted in Fig. 2(a). In addition, Fig. 2(b) displays the associated effective (von Mises) stress field.

The second set of calculations was performed using the computational model of an isolated nucleus with nuclear envelope [Fig. 1(b)]. In the numerical results presented in Fig. 3, the nuclear elements were taken as linear elastic materials with the following material constants: $K_b = 1.8 \times 10^{-19}$ N·m and $K_{NL} = 13.6 \times 10^{-19}$ N·m, $E = 25$ Pa, $\nu = 0.49$. The predicted deformation field for the model including the nuclear envelope [Fig. 3(a)] suggested that the nuclear envelope undergoes significant bending and stretching, inducing a more diffused response to sharp indentation, as compared to the highly localized response exhibited by the model without the nuclear membrane [Fig. 2(a)]. In addition, the maximum effective (von Mises) stress, induced by the point loading, was significantly reduced when the nuclear envelope was included in the computational model.

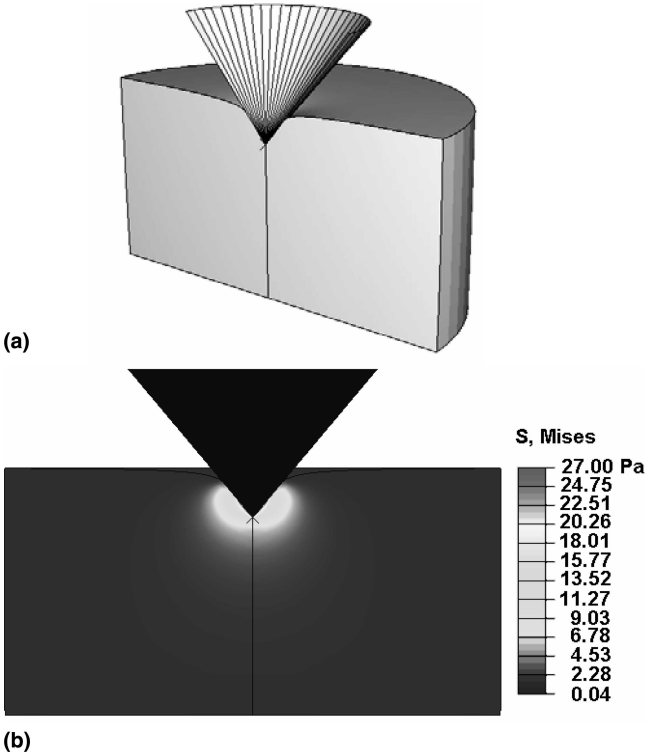

FIG. 2. (a) Displaced configuration and (b) effective (von Mises) stress field obtained using the computational model of an isolated nucleus excluding the nuclear envelope at the probe displacement of 1 μm. The height and radius of the axisymmetric model are equal to 5 μm. The nucleus is modeled as a linear elastic material with $E = 25$ Pa and Poisson's ratio of 0.49. The sharp probe has the half angle of 40°.

This comparative analysis emphasizes the importance of including the nuclear envelope in the computational model of a nucleus when sharp, pointed perturbations are considered. Furthermore, our simulations revealed that the pressure field is even more localized than the effective stress field in the model without the nuclear envelope, which leads to low sensitivity of the overall response on the material Poisson's ratio, contrary to the behavior of the model with nuclear envelope (see Sec. IV. B).

B. Influence of the stiffness of nucleoplasm, nuclear lamina, and nuclear membranes

Computational simulations were performed to explore the role of each individual nuclear element on the overall response of an isolated nucleus in sharp probe AFM indentation by systematically varying the elastic modulus of the nucleoplasm and the bending stiffness of the nuclear lamina and the nuclear membranes (Fig. 4). In this set of calculations, all the nuclear elements were taken as linear elastic materials with baseline elastic

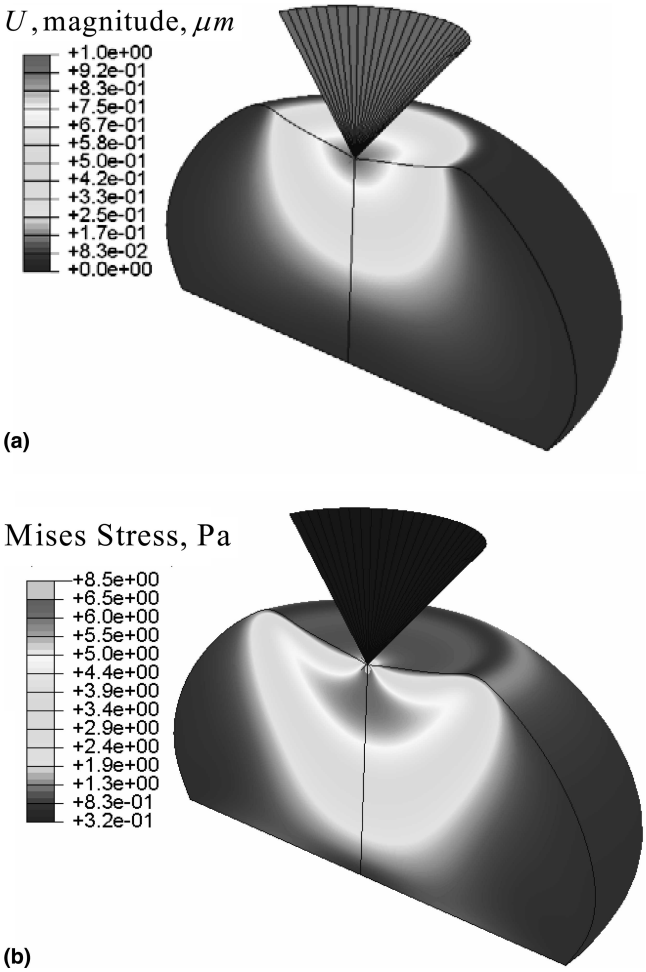

FIG. 3. (a) Nodal displacement field and (b) effective (von Mises) stress field in the nucleoplasm at the probe displacement of 1 μm obtained using the computational model of an isolated nucleus presented in Fig. 1. The nucleoplasm is modeled as a linear elastic material with E = 25 Pa. The computations are performed for the following material parameters of the nuclear membrane: $K_b = 1.8 \times 10^{-19}$ N·m and $K_{NL} = 13.6 \times 10^{-19}$ N·m. All the nuclear elements have equal Poisson's ratio of $\nu = 0.49$. The sharp probe has the half angle of 40°.

properties of $E = 25$ Pa, $K_b = 1.8 \times 10^{-19}$ N·m and $K_{NL} = 3.5 \times 10^{-19}$ N·m, $\nu = 0.485$. The computations were carried out for the half probe angle of $\alpha = 35°$, consistent with our indentation experiments. The force–indentation response of an isolated nucleus calculated using the computational model excluding the nuclear envelope (see Sec. IV. A) is also depicted in Fig. 4(a).

The average response, attained from AFM indentation experiments on 23 isolated nuclei extracted from mouse embryo fibroblasts, at constant indentation rate of 9 μm/s is also depicted in Fig. 4. Our experimental results revealed that the overall response of isolated nuclei exhibits little sensitivity to indentation rate, varied in the range of 0.4–9.0 μm/s (data not shown), implying a highly elastic response in this range of indentation rate, which is

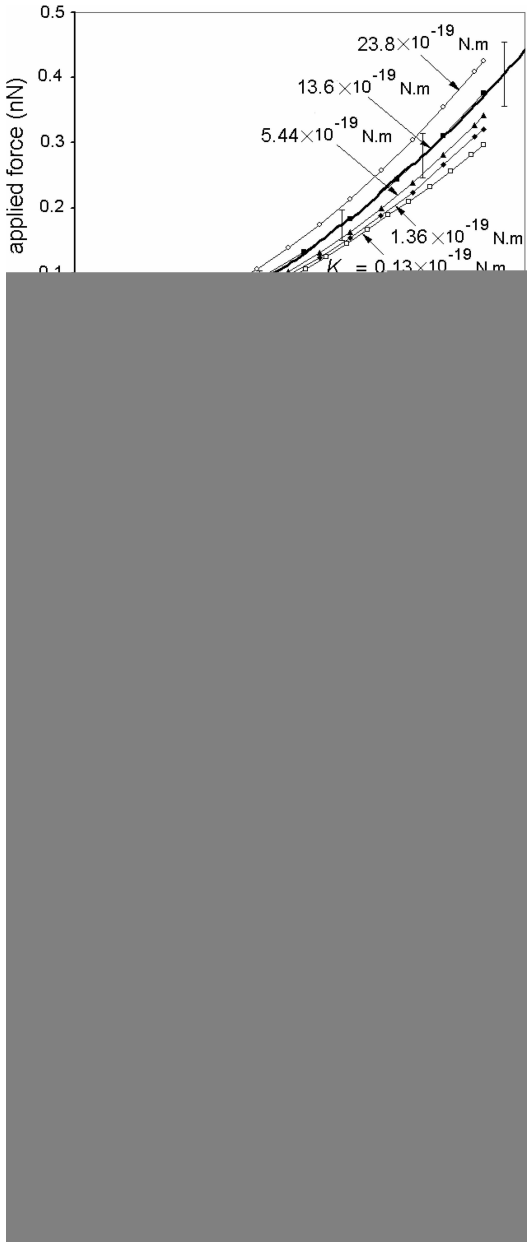

FIG. 4. Dependence of the force–indentation response of an isolated nucleus on the material properties of the nuclear elements. Panels (a) and (b) display the influence of bending stiffness of the nuclear lamina and lipid bilayer on the overall response of the isolated nucleus, respectively. Panel (c) shows the role of nucleoplasm elastic modulus on the overall response of the isolated nucleus. In panel (a) the response obtained using the computational model of an isolated nucleus excluding the nuclear envelope is also depicted ($E = 25$ Pa, $\nu = 0.485$). Here, all the nuclear elements are modeled as linear elastic material with Poisson's ratio of $\nu = 0.485$. In each set of calculations, the elastic properties associated with two of the nuclear elements are set to be equal to the baseline properties ($E = 25$ Pa, $K_b = 1.8 \times 10^{-19}$ N·m, $K_{NL} = 3.5 \times 10^{-19}$ N·m), and the stiffness of the third nuclear element is varied systematically. The experimental result (solid line) corresponds to the average response of 23 nuclei isolated from mouse embryo fibroblasts. The error bars represent the standard error of the data at specific values of indentation. In the computational simulations, the sharp probe has the half angle of 35°, which is consistent with the experiments.

consistent with the experimental observations on nuclei extracted from endothelial cells[25] and the particle-tracking measurement on fibroblasts nuclei.[27] The upper limit of $K_b = 1 \times 10^{-18}$ N·m for the bending stiffness of lipid bilayers was considered based on the results suggested by Zhelev et al.[38] for the membrane stiffness of neutrophils. The results presented in Fig. 4(a), associated with the role of nuclear lamina bending stiffness on the overall response of an isolated nucleus, cover a wide range of stiffness values, which was adopted based on our previous findings using isolated nuclei extracted from fibroblasts.

The results presented in Fig. 4 shed light on the structural role of nuclear elements in indentation experiments. As expected, the force–displacement response of the nucleus is highly sensitive to the elastic modulus of the nucleoplasm. In addition, the overall response of the nucleus shows higher sensitivity to the bending stiffness of nuclear membranes than to the nuclear lamina bending stiffness. It is noteworthy that the nuclear membranes tend to have a higher stretching stiffness than the nuclear lamina. It must be remarked that including the nuclear envelope in the computational model not only alters the overall response of the system [note that the prediction from the computational model excluding the nuclear envelope significantly underestimates the stiffness; Fig. 4(a)] but also defines the underlying mechanisms of deformation. The computational model without membrane fails to capture the main features of the response in indentation experiments, as discussed in Sec. IV. B and further emphasized in Sec. IV. D by studying the effect of probe angle on the overall response of an isolated nucleus.

The contact conditions between the inner membrane and outer membrane and also between the nuclear lamina and the inner nuclear membrane are between uncertainties in the computational model. As discussed in Sec. II, we speculated that the outer and inner nuclear membranes are free to slide relative to each other without friction. The other extreme case is a no slip condition between these two layers. We found that this contact condition yields a maximum 6% increase in reaction force exerted on the AFM probe at 1-μm indentation with the range of material properties and loading conditions studied here. Similarly, the effect of contact condition between the nuclear lamina and the inner nuclear membrane is examined by considering a free slip condition. The results indicate that this condition results in a maximum 8% reduction in peak reaction force exerted on the AFM probe in the range of this study. It is noteworthy that these contact conditions have a minimal effect on the effective stretching stiffness of the nuclear envelope, while they alter its bending stiffness significantly. However, in our study, the indentations were significantly larger than the nuclear envelope thickness, and therefore the structural resistance of the nuclear envelope was mainly attributed to its stretching stiffness.

A set of calculations was performed to study the role of nuclear elements' Poisson's ratios on the overall response of an isolated nucleus under sharp probe indentation. The results indicate that the curvature of the force–displacement response exhibits a remarkable sensitivity to the nuclear elements' Poisson's ratio, which is consistent with analogous studies on polymer thin films.[39] This is mainly attributed to the induced pressure field, which has a considerable contribution on the overall response of the nucleus as the material model reaches the limit of incompressibility.

C. Influence of the nucleoplasm viscosity and indentation rate

In this section, the role of nucleoplasm viscosity was examined on the overall response of an isolated nucleus under sharp probe indentation by systematically varying the characteristic time associated with the nucleoplasm material model between 0.1 and 2 s. In addition, the sensitivity of the nucleus overall response to indentation rate was studied. In both sets of calculations, the baseline elastic properties of the nuclear elements were taken as $E = 25$ Pa, $K_b = 1.8 \times 10^{-19}$ N·m, and $K_{NL} = 3.5 \times 10^{-19}$ N·m, $\nu = 0.485$. The effective creep strain fields were studied to gain some insight into the influence of viscosity on the response of an isolated nucleus in sharp probe indentation experiment.

Figure 5 displays the dependence of force–displacement response of the nucleus on the nucleoplasm characteristic time for the indentation velocity of 1 μm/s. The results associated with the nucleus model with elastic nucleoplasm are also plotted. The effective (von Mises) stress field and the effective creep strain field obtained from the computational models with nucleoplasm characteristic times of 0.1 and 2 s at indention of 1 μm are shown in Figs. 5(b) and 5(c), respectively. The effective creep strain field associated with the nucleus model with the nucleoplasm characteristic time of 0.1 s exhibited high values exceeding 0.25, while no significant creeping was evident for the nucleus model with the nucleoplasm characteristic time of 2 s at indentation depth of 1 μm.

The role of indentation rate on the force–displacement response of an isolated nucleus in sharp probe indentation experiments is shown in Fig. 6(a). If the time course of indentation experiments is considerably longer than the characteristic time associated with the viscosity of the nucleoplasm, the response of the isolated nucleus under indentation is effectively influenced by the nucleoplasm viscosity. The effective stress and effective creep strain fields associated with the lowest and highest indentation rate studied at the probe displacement of 1 μm are depicted in Figs. 6(b) and 6(c), respectively.

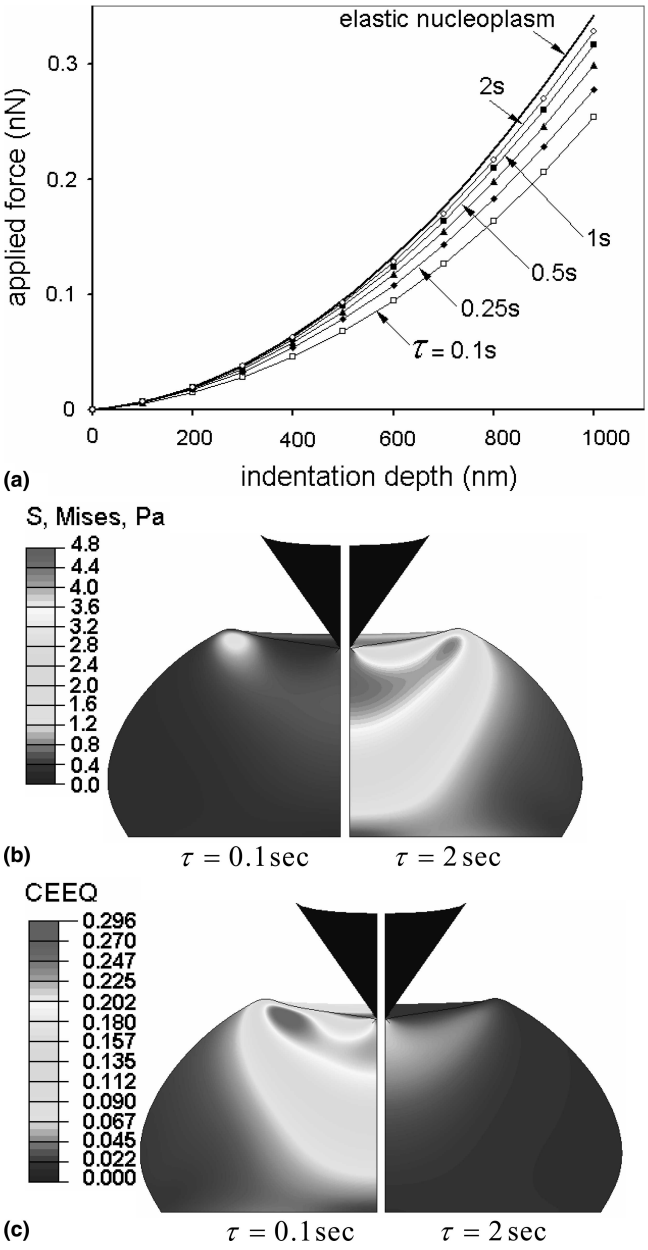

FIG. 5. (a) Force–indentation response of an isolated nucleus for various characteristic times associated with the viscous element of the nucleoplasm model. The nuclear envelope layers are modeled as linear elastic material with the $K_b = 1.8 \times 10^{-19}$ N·m and $K_{NL} = 3.5 \times 10^{-19}$ N·m. The nucleoplasm is modeled as viscoelastic Maxwell material with $E = 25$ Pa. All the nuclear elements have the same value of Poisson's ratio, $\nu = 0.485$. Comparison of the effective (von Mises) stress field and the effective creep strain field in the nucleoplasm for two characteristic times associated with the viscous element of the nucleoplasm model (0.1 and 2 s) at the probe displacement of 1 μm are displayed in (b) and (c), respectively. In the computational simulation, the sharp probe has the half angle of 35° and the indentation rate is 1 μm/s.

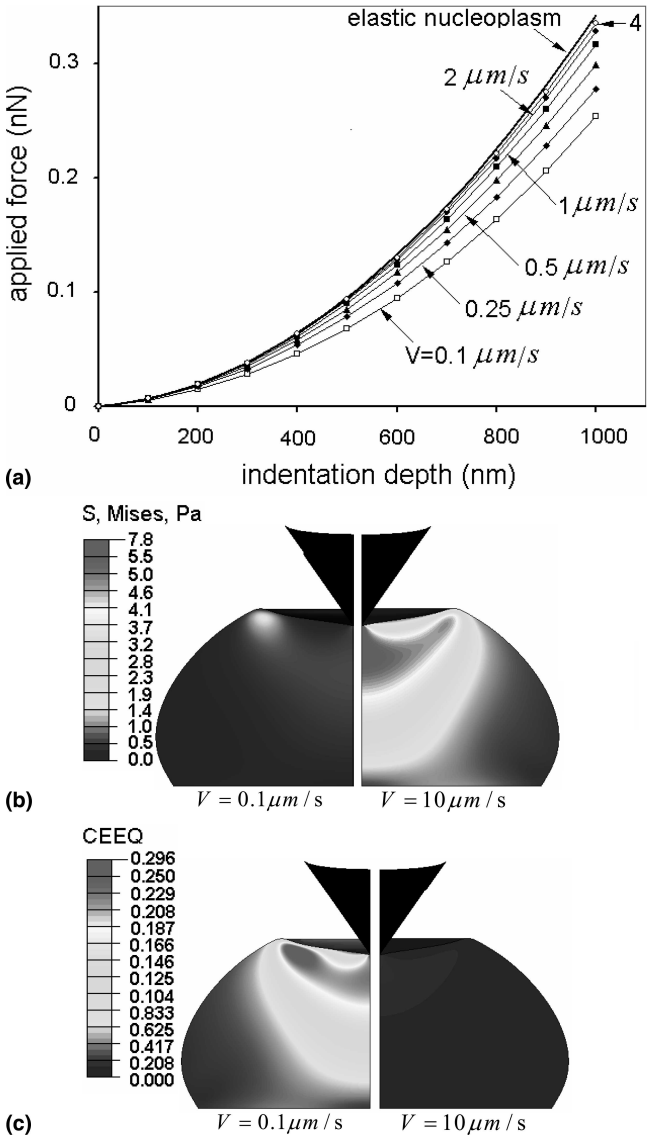

FIG. 6. (a) Force–indentation response of an isolated nucleus at various indentation rates. The nuclear envelope layers are modeled as linear elastic material with $K_b = 1.8 \times 10^{-19}$ N·m and $K_{NL} = 3.5 \times 10^{-19}$ N·m. The nucleoplasm is modeled as viscoelastic Maxwell material with $E = 25$ Pa and $\tau = 1$ s. All the nuclear elements have $\nu = 0.485$. Comparison of the effective (von Mises) stress field and the effective creep strain field in the nucleoplasm for two indentation rates (0.1 and 10 μm /s) at the probe displacement of 1 μm are presented in (b) and (c), respectively. The sharp probe has the half angle of 35°.

D. Influence of the probe angle

A set of calculations was performed to explore the role of sharp probe angle on the force–displacement response of a nucleus in indentation experiments. In the calculations, all the nuclear elements were taken to be linear elastic material with constant Poisson's ratio, $\nu = 0.485$ and the baseline elastic properties of $E = 25$ Pa, $K_b = 1.8 \times 10^{-19}$ N·m and $K_{NL} = 3.5 \times 10^{-19}$ N·m. Figure 7(a) shows the force–displacement response of an isolated nucleus under sharp probe indentation with various half angles, α. The results indicated that the force–displacement response of the nucleus model does not exhibit a considerable sensitivity to the probe half angle, as long as the probe is not nearly flat; the sharp probe

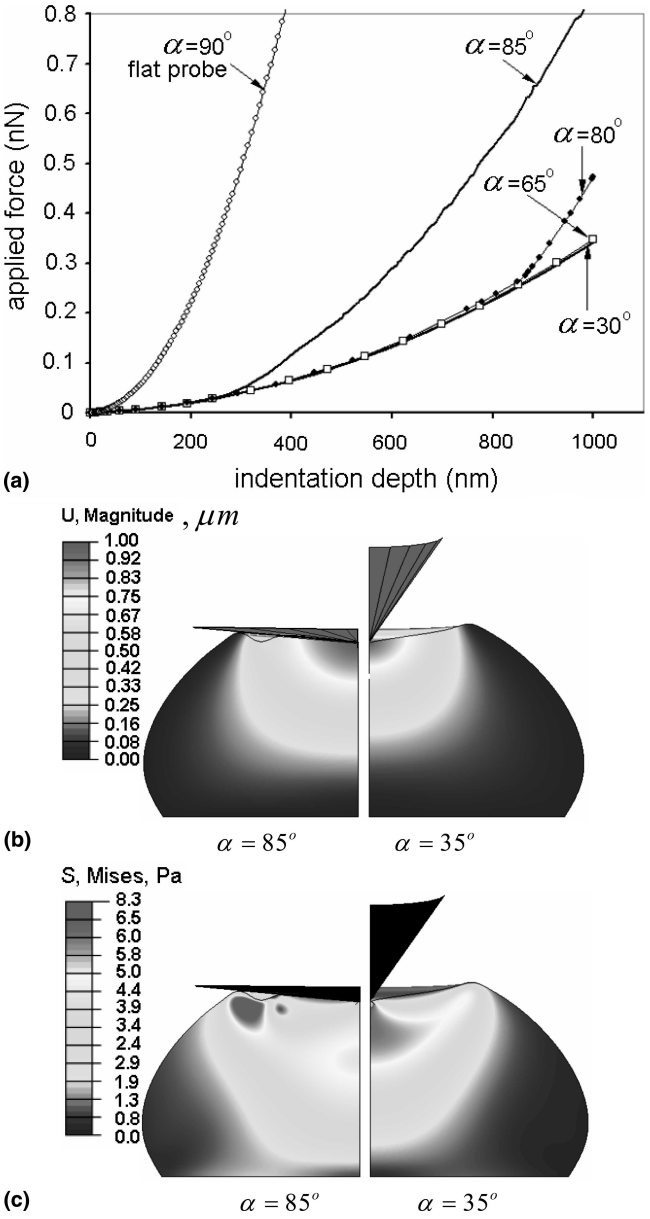

FIG. 7. (a) Force–indentation response of an isolated nucleus for various half angles of the sharp probe, α. All the nuclear elements are modeled as linear elastic material with $E = 25$ Pa, $K_b = 1.8 \times 10^{-19}$ N·m, $K_{NL} = 3.5 \times 10^{-19}$ N·m, and $\nu = 0.485$. (b) The nodal displacement field and (c) the effective (von Mises) stress field in the nucleoplasm at the probe displacement of 1 μm for two probe half angles of 35° and 85°.

indentation is effectively a point load and the current calculations suggest that the nuclear membrane undergoes bending and stretching, which induces a diffuse response to sharp indentation, as compared to the localized response exhibited by a model lacking the nuclear membrane. This further emphasizes the necessity of considering the nuclear envelope in the computational model. For probe angle of $\alpha = 80°$, a sudden change in the apparent stiffness (force–displacement response slope) is evident at the probe displacement of $\delta \approx 0.85$ μm, as a part of the nuclear envelope makes contact with the probe. Further increase in the probe angle leads to a drastic alteration in the deformation mechanism and the associated response. For a nearly flat probe, the displacement field appears more diffuse and the effective stress field in the nucleoplasm exhibits an utterly dissimilar pattern to that observed under sharp probe indentation with probe angle of $\alpha < 65°$ [Figs. 7(b) and 7(c)]. Local buckling of the nuclear envelope underneath the probe is evident for indentation with an almost-flat probe, which is in contrast to indentation with a sharp probe having $\alpha < 80°$, in which no membrane buckling is predicted and the nuclear envelope undergoes stretching and bending during deformation. The distribution of the effective (von Mises) stress is also remarkably different for the two cases mentioned above [Fig. 7(c)]. The present computational results indicate that the response of an isolated nucleus in indentation experiments with flat or almost flat probes is highly sensitive to the exact probe geometry and therefore should be interpreted by caution. In addition, other phenomena such as sliding relative to the substrate might play an important role on indentation with almost flat probes.

V. CONCLUDING REMARKS

The results presented here emphasize the importance of employing a robust biomechanical model for studying the mechanisms driving the mechanical response of nucleus and stress distribution in the nuclear elements under mechanical stimuli. The nucleus model without a membrane clearly failed to capture the main features of the experimental indentation response. It is noteworthy that in the Hertzian contact model, which has been used in many studies for interpreting the experimental observation from indentation experiments on cells and nuclei, the force–displacement response of the material under indentation is strongly dependent on the probe angle; e.g., the force predicted for a probe with half angle of $\alpha = 80°$ is approximately eight times higher than the force associated with the probe with half angle of $\alpha = 35°$ at the same level of indentation. In contrast, our numerical simulations revealed that the overall response of an isolated nucleus, as well as the underlying mechanisms of deformation, is not sensitive to the probe angle, as long as the probe is not almost flat. This has another immediate implication: the parametric analyses, carried out to study the nuclear mechanics in indentation with sharp probe with half angle of $\alpha = 35°$, are valid for a large range of indentation experiments (as long as the probe is not nearly flat). It is noteworthy that the finite dimensions of the computational model could affect the overall response of the isolated nucleus and the associated stress distributions, which underscores the need for accurately

visualizing the isolated nucleus before generating the computational models. In addition, in our experiments the nucleus was placed freely on (i.e., not adhered to) the substrate with minimal pre-stress. It is conceivable that the tensile stress induced along the membrane by adhering the nucleus to substrate could considerably enhance the apparent stiffness of the nucleus in indentation.[40] Recent observations by Deguchi et al. suggest that membrane-bound organelles may locally compress the nucleus, and the mechanical stresses transmitted by these local perturbations might alter the function of the nucleus as well as its morphology.[10] Our results suggest that the local mechanical perturbation of a nucleus surface may lead to a diffused response and mitigation of the intracellular stress.

The computational model studied here in combination with rigorous experimental observations, employing various techniques, could lead to a general protocol for studying the nuclear mechanics under mechanical stimuli. This general protocol allows the mechanical properties of each individual nuclear element to be ascertained. It may also help to identify the effects of various kinds of mutations and gene alteration on nuclear mechanics and to develop a better understating in analyzing tissue-specific effects of the mutations in promoting particular diseases.

ACKNOWLEDGMENTS

We thank Dr. Roger D. Kamm, Dr. Zhenyu Xue, and Dr. John W. Hutchinson for many valuable discussions and Dr. Richard Lee and Dr. Jan Lammerding for their assistance with the experimental protocol. We are also thankful to anonymous referees for rigorous review of this manuscript and valuable suggestions. This work has been supported in part by the Division of Engineering and Applied Sciences, Harvard University, Cambridge, MA.

REFERENCES

1. U. Aebi, J. Cohn, L. Buhle, and L. Gerace: The nuclear lamina is a meshwork of intermediate-type filaments. *Nature* **323,** 560 (1986).
2. C.J. Hutchison: Lamins: Building blocks or regulators of gene expression? *Nat. Rev. Mol. Cell Biol.* **3,** 848 (2002).
3. J.W. Newport and D.J. Forbes: The nucleus: Structure, function, and dynamics. *Annu. Rev. Biochem.* **56,** 535 (1987).
4. P.F. Davies: Flow-mediated endothelial mechanotransduction. *Physiol. Rev.* **75,** 519 (1995).
5. D.E. Ingber: Tensegrity: The architectural basis of cellular mechanotransduction. *Annu. Rev. Physiol.* **59,** 575 (1997).
6. P.A. Janmey: The cytoskeleton and cell signaling: Component localization and mechanical coupling. *Physiol. Rev.* **78,** 763 (1998).
7. G. Dai, N.R. Kaazempur-Mofrad, S. Natarajan, Y. Zhang, S. Vaughn, B.R. Blackman, R.D. Kamm, G. Garcia-Cardena, and M.A. Gimbrone, Jr.: Distinct endothelial phenotypes evoked by arterial waveforms derived from atherosclerosis-susceptible and -resistant regions of human vasculature. *Proc. Natl. Acad. Sci. USA* **101,** 14871 (2004).
8. K.N. Dahl, S.M. Kahn, K.L. Wilson, and D.E. Discher: The nuclear envelope lamina network has elasticity and a compressibility limit suggestive of a molecular shock absorber. *J. Cell Sci.* **117,** 4779 (2004).
9. J. Lammerding, P.C. Schulze, T. Takahashi, S. Kozlov, T. Sullivan, R.D. Kamm, C.L. Stewart, and R.T. Lee: Lamin A/C deficiency causes defective nuclear mechanics and mechanotransduction. *J. Clin. Invest.* **113,** 370 (2004).
10. S. Deguchi, K. Maeda, T. Ohashi, and M. Sato: Flow-induced hardening of endothelial nucleus as an intracellular stress-bearing organelle. *J. Biomech.* **38,** 1751 (2005).
11. A. Vaziri and M.R. Kaazempur-Mofrad: A computational study on the nuclear mechanics and deformation in micropipette aspiration experiment (2006, unpublished).
12. F. Guilak, J.R. Tedrow, and R. Burgkart: Viscoelastic properties of the cell nucleus. *Biochem. Biophys. Res. Commun.* **269,** 781 (2000).
13. P. Lemoine and J.M. McLaughlin: Nanomechanical measurements on polymers using contact mode atomic force microscopy. *Thin Solid Films* **339,** 258 (1999).
14. S.N. Magonov and D.H. Reneker: Characterization of polymer surfaces with atomic force microscopy. *Annu. Rev. Mater. Sci.* **27,** 175 (1997).
15. M.R. VanLandingham, R.R. Dagastine, R.F. Eduljee, R.L. McCullough, and J.W. Gillespie: Characterization of nanoscale property variations in polymer composite systems: 1. Experimental results. *Composites A* **30,** 75 (1999).
16. H. Shulha, A. Kovalev, N. Myshkin, and V.V. Tsukruk: Some aspects of AFM nanomechanical probing of surface polymer films. *Eur. Polym. J.* **40,** 949 (2004).
17. K. Efimenko, M. Rackaitis, W. Manias, A. Vaziri, L. Mahadevan, and J. Genzer: Nested self-similar wrinkling patterns in skins. *Nat. Mater.* **4,** 293 (2005).
18. J. Domke and M. Radmacher: Measuring the elastic properties of thin polymeric films with the atomic force microscope. *Langmuir* **14,** 3320 (1998).
19. P.M. McGuiggan and D.J. Yarusso: Measurement of the loss tangent of a thin polymeric films using the atomic force microscopy. *J. Mater. Res.* **19,** 387 (2004).
20. Y.Y. Lim, M.M. Chaudhri, and Y. Enomoto: Accurate determination of the mechanical properties of thin aluminum films deposited on sapphire flats using nanoindentations. *J. Mater. Res.* **14,** 2314 (1999).
21. M. Bezanilla, B. Drake, E. Nudler, M. Kashlev, P.K. Hansma, and H.G. Hansma: Motion and enzymatic degradation of DNA in the atomic force microscope. *Biophys. J.* **67,** 2454 (1994).
22. J.H. Hoh and C.A. Schoenenberger: Surface morphology and mechanical properties of MDCK monolayers by atomic force microscopy. *J. Cell Sci.* **107,** 1105 (1994).
23. R.E. Mahaffy, C.K. Shih, F.C. MacKintosh, and J. Kas: Scanning probe-based frequency-dependent microrheology of polymer gels and biological cells. *Phys. Rev. Lett.* **85,** 880 (2000).
24. M. Radmacher, M. Fritz, C.M. Kacher, J.P. Cleveland, and P.K. Hansma: Measuring the viscoelastic properties of human platelets with the atomic force microscope. *Biophys. J.* **70,** 556 (1996).
25. N. Caille, O. Thoumine, Y. Tardy, and J.J. Meister: Contribution of the nucleus to the mechanical properties of endothelial cells. *J. Biomech.* **35,** 177 (2002).
26. K.N. Dahl, A.J. Engler, J.D. Pajerowski, and D.E. Discher: Power-law rheology of isolated nuclei with deformation mapping of nuclear sub-structures. *Biophys. J.* (2005).

27. Y. Tseng, J.S. Lee, T.P. Kole, I. Jiang, and D. Wirtz: Micro-organization and visco-elasticity of the interphase nucleus revealed by particle nanotracking. *J. Cell Sci.* **117,** 2159 (2004).
28. T. Senda, A. Iizuka-Kogo, and A. Shimomura: Visualization of the nuclear lamina in mouse anterior pituitary cells and immunocytochemical detection of lamin A/C by quick-freeze freeze-substitution electron microscopy. *J. Histochem. Cytochem.* **53,** 497 (2005).
29. G. Schatten and M. Thoman: Nuclear surface complex as observed with the high resolution scanning electron microscope. Visualization of the membrane surfaces of the neclear envelope and the nuclear cortex from Xenopus laevis oocytes. *J. Cell Biol.* **77,** 517 (1978).
30. B. Burke and C.L. Stewart: Life at the edge: The nuclear envelope and human disease. *Nat. Rev. Mol. Cell Biol.* **3,** 575 (2002).
31. N.M. Maraldi, G. Lattanzi, S. Marmiroli, S. Squarzoni, and F.A. Manzoli: New roles for lamins, nuclear envelope proteins and actin in the nucleus. *Adv. Enzyme Regul.* **44,** 155 (2004).
32. C. Ostlund and H.J. Worman: Nuclear envelope proteins and neuromuscular diseases. *Muscle Nerve* **27,** 393 (2003).
33. H. Karcher, J. Lammerding, H. Huang, R.T. Lee, R.D. Kamm, and M.R. Kaazempur-Mofrad: A three-dimensional viscoelastic model for cell deformation with experimental verification. *Biophys. J.* **85,** 3336 (2003).
34. N. Mohandas and E. Evans: Mechanical properties of the red cell membrane in relation to molecular structure and genetic defects. *Annu. Rev. Biophys. Biomol. Struct.* **23,** 787 (1994).
35. O. Thoumine, A. Ott, O. Cardoso, and J.J. Meister: Microplates: A new tool for manipulation and mechanical perturbation of individual cells. *J. Biochem. Biophys. Methods* **39,** 47 (1999).
36. G.G. Bilodeau: Regular pyramid punch problem. *J. Appl. Mech. Trans. ASME* **59,** 519 (1992).
37. H. Hertz: On the contact of solid flexible bodies. *J. reine angewandte Math.* **92,** 156 (1881).
38. D.V. Zhelev, D. Needham, and R.M. Hochmuth: Role of the membrane cortex in neutrophil deformation in small pipets. *Biophys. J.* **67,** 696 (1994).
39. R.E. Mahaffy, S. Park, E. Gerde, J. Kas, and C.K. Shih: Quantitative analysis of the viscoelastic properties of thin regions of fibroblasts using atomic force microscopy. *Biophys. J.* **86,** 1777 (2004).
40. A. Hategan, R. Law, S. Kahn, and D.E. Discher: Adhesively-tensed cell membranes: Lysis kinetics and atomic force microscopy probing. *Biophys. J.* **85,** 2746 (2003).